Article ID: 1003－6326(2004)04－0665－05

Crystallization process in rapidly solidified Al-Nd-Ni amorphous alloy prepared by melt spinning①

XIAO Yu-de(肖于德), LI Wen-xian(黎文献), MA Zheng-qing(马正青)
(School of Materials Science and Engineering, Central South University, Changsha 410083, China)

Abstract: Rapidly solidified ribbons of $Al_{90}Nd_7Ni_3$ metallic glasses were prepared by using melt spinning. Crystallization process of the totally amorphous ribbons was investigated by differential scanning calorimetry and X-ray diffraction analysis, under continuous heating regime. The results show that, under continuous heating regime, the metallic glass devitrifies via two main stages: primary crystallization, resulting in two-phase mixture of α(Al) plus residual amorphous phase, and secondary crystallization, corresponding to some inter-metallic phases appearing, successively including $Al_{11}Nd_3$, Al_3Ni, and some unknown phases, in the Al amorphous/crystal matrix. Four peaks appear on the continuous heating DSC curves. Their peak temperatures are respectively 470.8, 570.8, 585.6, and 731.6 K at infinitesimal heating rate, and their activation energies of the respective phase transformation are 183.0, 294.7, 232.5 and 269.1 kJ/mol. The values of Avrami exponent of the four reactions decrease with increasing relative transformation degree. At the earlier stage of phase transformation, the values of n are larger than 4, and at the later stage the values of n become close to some value from 0.5 to 2.0.

Key words: rapid solidification; Al-riched amorphous alloy; crystallization process; phase transformation
CLC number: TG 146.2 **Document code:** A

1 INTRODUCTION

In the recent few years, Al-rich metallic glass has been paid more and more attention to in the novel materials research field, not only due to its high strength, hardness and low density, but also because a new-type Al-based nanophase composite can be obtained from it by partial crystallization[1-7].

Many Al-based amorphous/nanocrystalline alloys containing rare earth(RE= La, Y, Ce, Nd, etc) and transition metal(TM = Fe, Co, Ni, etc) elements have an attractive combination of mechanical properties. It has been reported that many of these Al-based amorphous alloys exhibit high tensile strength above 950－1 150 MPa. It has been subsequently found that the nanophase composites produced via partial crystallization of the metallic glasses can have a significantly improved tensile strength, up to 1 560 MPa, about 1.5 times as high as that of the corresponding fully amorphous alloy and about 3 times as high as that of conventional dispersion-strengthened Al alloy. It is indicated that partial crystallization of Al-rich metallic glass may be an effective way to obtain novel lightmass structural materials with high strength and good ductility[1-17]. However, many careful studies ought to be done firstly to understand the overall crystallization process of Al-based fully amorphous alloys.

Therefore, the purpose of the present paper is to study the thermal behavior and phase transformation during crystallization of rapidly solidified $Al_{90}Nd_7Ni_3$ amorphous alloy, by using differential scanning calorimetry and X-ray diffraction examination.

2 EXPERIMENTAL

Rapidly solidified ribbons were prepared in a single copper roll melt-spinner after melted with high pure Al, Nd, and Ni. The ribbons are typically less than 3 mm wide and 30 μm thick, with chemical composition of $Al_{90}Nd_7Ni_3$(mole fraction).

Differential scanning calorimetric curves were obtained in an Ar atmosphere by using a Perkin-Elmer DSC-7. The samples were heated continuously up to 850 K at various heating rates of 2.5, 5, 10, 20, 40, 60 and 80 K/min.

Phase identification and structural characterization of the as-spun and annealed (partialy or fully) ribbons was done by conventional X-ray diffraction (XRD), which was performed in a SIEMENS D500 X-ray diffrationmeter with monochromatic CuK_α radiation(λ= 0.154 18 nm) over a 2-theta angle range of 30°－50° at a step of 0.03°.

① **Foundation item:** Project(G1999064900) supported by the National Basic Research Program of China
Received date: 2003－12－30; **Accepted date:** 2004－05－11
Correspondence: XIAO Yu-de, PhD; Tel: +86-731-8830261; E-mail: xiaoyude@mail.csu.edu.cn

3 RESULTS AND DISCUSSION

3.1 Exothermic transformation during crystallization of $Al_{90}Nd_7Ni_3$ metallic glass under continuous heating regime

Fig. 1 shows the DSC curve for heating rate of 2.5 K/min. Four exothermal peaks are observed in the temperature range from 300 to 850 K on the curve.

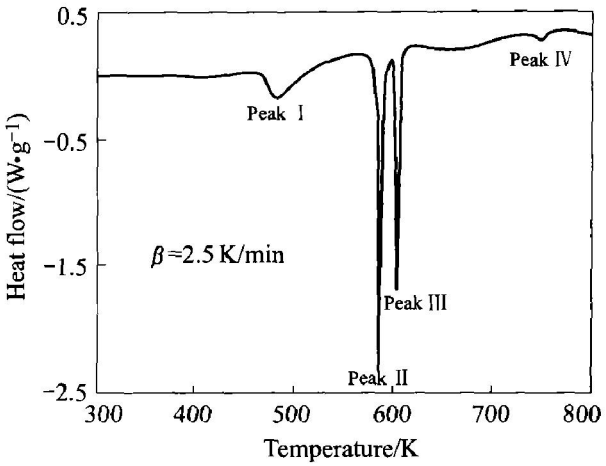

Fig. 1 DSC curve of $Al_{90}Nd_7Ni_3$ metallic glass at heating rate of 2.5 K/min

The X-ray diffraction patterns for the as-quenched $Al_{90}Nd_7Ni_3$ ribbon and its annealed ones exposed thermally at various temperatures for several minutes are shown in Fig. 2. The broad halo of the diffraction pattern obtained before DSC analysis indicates that the as-spun ribbon has full amorphous structure without appreciable crystalline phase. The other diffraction patterns show that, Al is the only crystalline phase in the samples heated at the lower temperatures, whereas Al, $Al_{11}Nd_3$ and Al_3Ni phases exist in the samples annealed above 625 K, and even other unknown phases appearing at higher temperature. The unknown phases may be a binary intermetallic compound with crystal structure of Al_3Y[18], or be a ternary intermetallic phase with crystal structure of $Al_{16}Ni_3Y$[19]. However, more careful research ought to be done further to identify them in the future.

The DSC and XRD results indicate that the crystallization process of the as-quenched $Al_{90}Nd_7Ni_3$ ribbon is divided into two main stages: precipitation of Al phase followed by forming of some intermetallic compounds, which is consistent with other experimental work on Al-based amorphous alloys[9, 20].

3.2 Characteristic temperature, mean activation energy of crystallization of $Al_{90}Nd_7Ni_3$ metallic glass under continuous heating regime

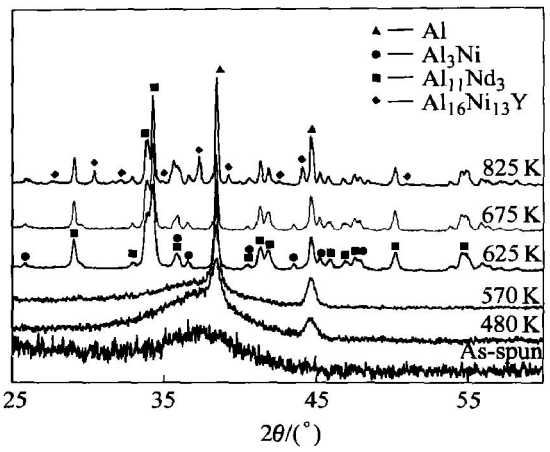

Fig. 2 X-ray diffraction patterns for annealed ribbons of $Al_{90}Nd_7Ni_3$ metallic glass at various temperatures

Fig. 3 exhibits the variation of the onset temperature, T_{on}, and the peak temperature, T_p of the four DSC peaks with heating rate for the as-quenched $Al_{90}Nd_7Ni_3$ ribbon. It can be seen that, both T_{on} and T_p are elevated with heating rate improving. By extrapolation of these plots to heating rate being zero, the values of T_{on} and T_p at infinitesimal heating rate are determined to be respectively 456.5 and 470.8 K for Peak I, 567.2 and 570.8 K for Peak II, 582.6 and 585.6 K for Peak III, and 720.6 and 731.6 K for Peak IV.

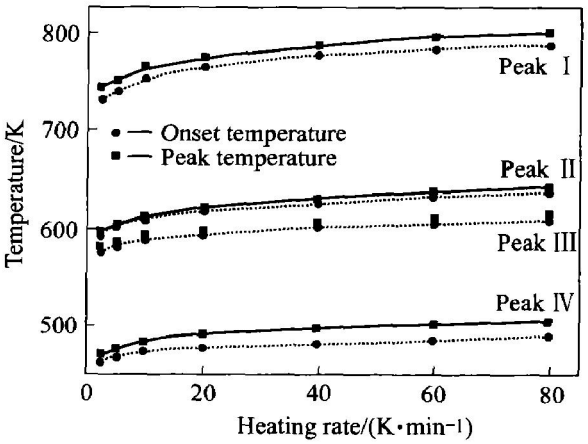

Fig. 3 Variation of T_{on} and T_p of four DSC peaks with heating rate

The Johnson-Mehl-Avrami-Kolmogorov Equation(JMAK) is the most widely used approach for the description of isothermal reaction,

$$X = 1 - \exp(-kt^n) \quad (1)$$

where X is the relative reaction degree as a function of time at the given temperature; n, the Avrami exponent, depending on rate of nucleation and morphology of growth during the reaction, and k is the Avrami reaction rate constant, depending on thermal history of the samples.

However, to apply the JMAK Equation to describe the non-isothermal reaction, it is necessary to take into account the dependence of k on time, t. Thus[18, 19],

$$X = 1 - \exp\{-[\int_0^t k(T(t))\mathrm{d}t]^n\} \quad (2)$$

where k is associated with the reaction activation energy (E), J/mol, and the temperature, T in through the Arrhenius temperature dependence,

$$k(T) = v\exp(-E/(RT)) \quad (3)$$

where T is a function of time, $\mathrm{d}T = \beta\mathrm{d}t$, β is the heating rate in K/min, and v is frequency factor.

At a certain temperature (T_p), the reaction rate, $\mathrm{d}X/\mathrm{d}t$, reaches its maximum,

$$\left.\frac{\mathrm{d}^2X}{\mathrm{d}t^2}\right|_{T=T_p} = 0 \quad (4)$$

By taking the second derivation of Eqn. (2) and combining with Eqn. (4), the so-called Kissinger Equation relating the reaction kinetics parameters E to temperature, T_p, and heating rate, β can be finally derived[20],

$$\ln(T_p^2/\beta) = E/(RT_p) + \ln(E/(vR)) \quad (5)$$

According to Eqn. (5), a plot of $\ln(T_p^2/\beta)$ vs $1/T_p$ would be linear, and activation energy, E, can be easily determined from the slope of the plot, as given in Fig. 4. The activation energy E can also be calculated through another widely used non-isothermal method based on the so called Ozawa Equation[21],

$$\ln(1/\beta) = E/(RT_p) + C \quad (6)$$

where C is a constant. A plot of $\ln\beta$ versus $1/T_p$ is also shown in Fig. 5.

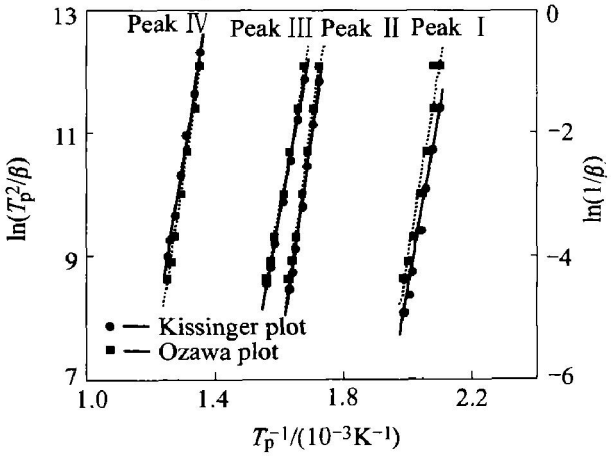

Fig. 4 Plots of $\ln(T_p^2/\beta)$ versus $1/T_p$ and of $\ln\beta^{-1}$ versus $1/T_p$

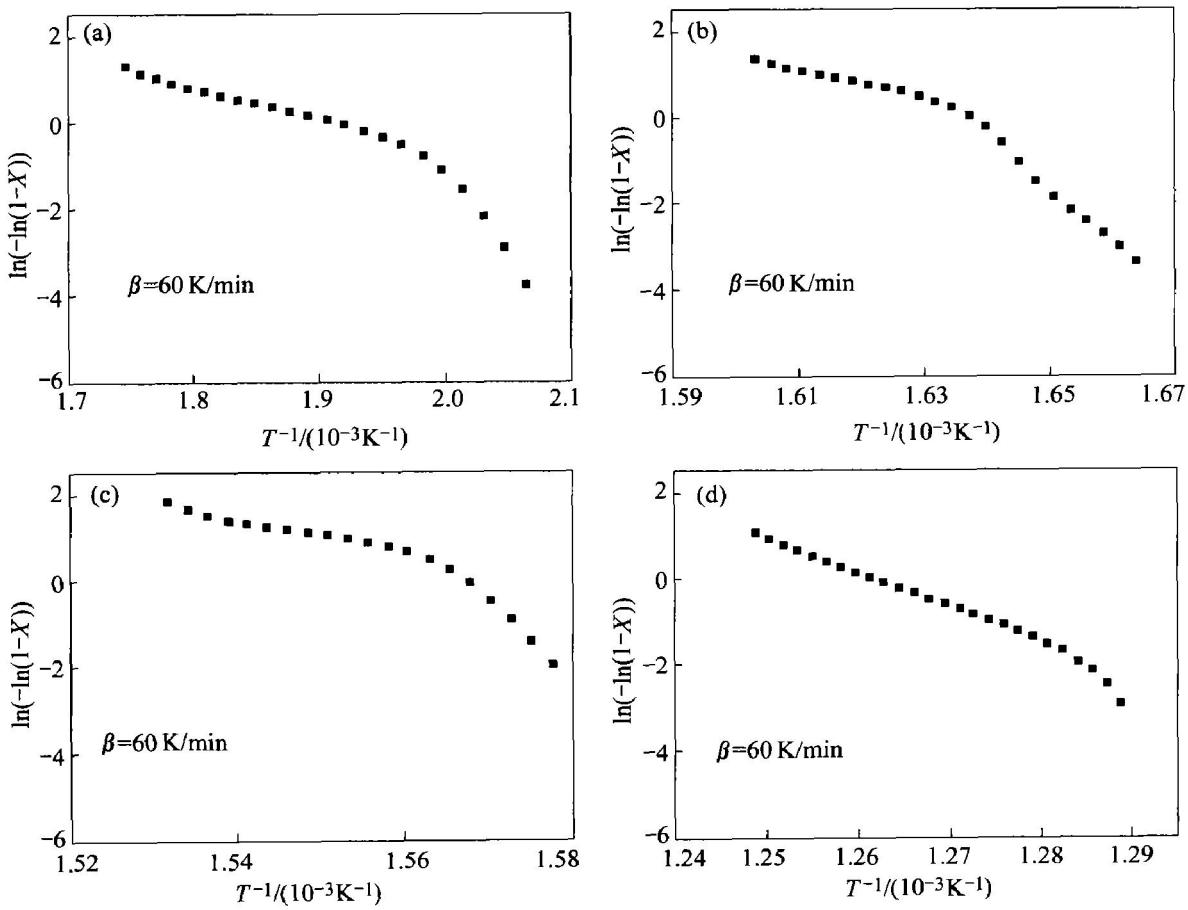

Fig. 5 Plots of $\ln[-\ln(1-X)]$ versus T^{-1} under continuous heating regimes
(a) —Peak I; (b) —Peak II; (c) —Peak III; (d) —Peak IV

The values of E determined by the two methods are summarized in Table 1. The activation energies calculated by the Kissinger and Ozawa Equations show good agreement, which indicates that the reaction order is close to unity.

Table 1 Activation energy (E) determined by Kissinger and Ozawa Equations(kJ·mol^{-1})

Peak	Eqn. (5)	Eqn. (6)
I	183.0	191.1
II	294.7	304.6
III	232.5	242.8
IV	269.1	281.9

3.3 Non-isothermal kinetics and Avrami exponent of crystallization of $Al_{90}Nd_7Ni_3$ metallic glass under continuous heating regime

The extent of reaction at any time is defined as[18, 19]

$$X = \Delta H / \Delta H_0 = [\int_{T_{on}}^{T} (\mathrm{d}H/\mathrm{d}T)\mathrm{d}T] / \Delta H_0 \quad (7)$$

where ΔH is the partial heat of reaction up to the temperature of interest, T, and ΔH_0 is the ultimate heat of reaction. Here it is thought that $X \approx A/A_0$, where A_0 is the overall area under the DSC curve between the temperature T_{on}, at which the reaction starts, and the temperature T_{en}, at which the reaction is completed, and A is the partial area bounded by T_{on} and T.

The integral in the Eqn. (2) can be evaluated by the alternating series[18, 19],

$$\int e^{-y}y^{-2}\mathrm{d}y = -e^{-y}y^{-2}\sum_{i=0}^{\infty}(-1)^i(i+1)!y^{-1} \quad (8)$$

where the substitution $y = E/RT$ is used, and the first three terms are available without any significant error for the calculation of n and E, and thus Eqn. (2) can be rewritten as

$$\ln[-\ln(1-X)] = n\ln(Rv/(\beta E)) + 2n\ln(T) - nE/(RT) + n\ln[1 - 2RT/E + 6(RT/E)^2] \quad (9)$$

If $E \gg RT$, Eqn. (9) can be changed into

$$\ln[-\ln(1-X)] \approx n\ln(v/\beta) + n\ln(RT^2/E) - nE/(RT) \quad (10)$$

Since the term $\ln(RT^2/E)$, will not vary strongly compared to E/RT in Eqn. (10), the $\ln[-\ln(1-X)]$ is dominated by the third term, nE/RT, and thus a plot of $\ln[-\ln(1-X]$ vs $1/T$ will give a straight line with the slope of nE/R. However, as a matter of fact, the plot of $\ln[-\ln(1-X)]$ vs $1/T$ does not exhibit a straight line, as shown in Fig. 5.

For the non-isothermal crystallization, the transformed fraction in the $Al_{90}Nd_7Ni_3$ metallic glass increase with heating temperature improving during continuous heating. Here the Avrami exponent, n, is calculated by the slope of $\ln[-\ln(1-X)]$ vs $1/T$ at a given temperature. Variation of the n value with the transformed fraction increasing is shown in Fig. 6. The values of Avrami exponent decrease with development of the reaction. It indicates that during the phase transformations nucleation rate and grown rate decrease with heating temperature and the reaction degree improving.

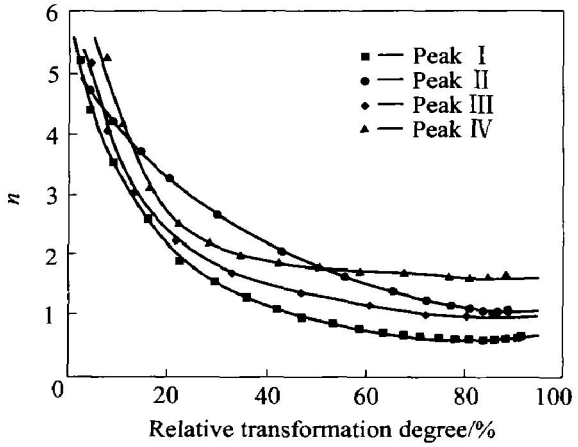

Fig. 6 Variation of value of Avrami exponent n with crystallized fraction increasing under continuous heating regime at 60 K/min

In particular, it should be pointed that, since $n = 4$ means that the phase transformation occurs in a three-dimensional mode with a constant nucleation rate[21-25], at the earlier stage of these phase transformations, corresponding to Peak I, II, III and IV, the values of n are larger than 4, as shown in Fig. 6, resulting from rapid increasing of nucleation rate, while at the later stage the values of n become constant, being close to 0.5 and 2.0, respectively, which implies that the phase transformations are controlled in a mode with a decreasing nucleation rate and a decreasing grown rate at the later stage of phase transformation.

4 CONCLUSIONS

1) Crystallization process of rapidly solidified $Al_{90}Nd_7Ni_3$ metallic glasses involves two main stages: primary crystallization, resulting in two-phase mixture of α(Al) plus residual amorphous phase, and secondary crystallization, corresponding to some inter-metallic phases appearing, successively including $Al_{11}Nd_3$, Al_3Ni, and even $Al_{16}Ni_3Nd$ and Al_3Nd, in the Al amorphous/crystal matrix.

2) There are four exothermic peaks on the DSC curve of $Al_{90}Nd_7Ni_3$ metallic glass under continuous heating regime. The peak temperatures of the four

peaks are respectively 470.8, 570.8, 585.6, and 731.6 K at infinitesimal heating rate, and activation energies of the respective phase transformation 183.0, 294.7, 232.5 and 269.1 kJ/mol, calculated by the Kissinger Method.

3) The values of Avrami exponent of the four reaction decrease with relative transformation degree increasing. At the earlier stage of phase transformation, the values of n are larger than 4, and at the later stage the values of n become close to some value from 0.5 to 2.0.

REFERENCES

[1] Greer A L. Metallic glasses[J]. Science, 1995, 267: 1947 - 1953.

[2] Das S K, Perepezko J H, Wu R I, et al. Undercooling and glass formation in Al-based alloys[J]. Mater Sci Eng 2001, A304 - 306(1): 159 - 168.

[3] Kim Y H, Soh J-R, Kim D K, et al. Glass formation in metallic Al-Ni-Y[J]. J Non-Crystalline Solids, 1998, 242(2 - 3): 122 - 130.

[4] Allen D R, Foley J C, Perepezko J H. Nanocrystal development during primary crystallization of amorphous alloys [J]. Acta Metallurgica et Materialia, 1998, 46(2): 431 - 440.

[5] Inoue A, Ohtera K, Kita K, et al. New amorphous alloys with good ductility in Al-Ce-M(M= Nb, Fe, Co, Ni or Cu) systems[J]. Jpn J Appl Phys, 1988, 27(8): 1796 - 1799.

[6] Inoue A, Ohtera K, Tsai A P, et al. Glass transition behavior of Al-Y-Ni and Al-Ce-Ni amorphous alloys[J]. Jpn J Appl Phys, 1988, 27(3): 280 - 282.

[7] He Y. Poon S J, Shifet G J. Synthesis and properties of metallic glasses that contain aluminum [J]. Science, 1988, 241: 1640 - 1642.

[8] Inoue A, Kimura H M, Sasamori K, et al. Synthesis and high mechanical strength of Al-based alloys consisting mainly of nanogranular amorphous particles[J]. Mater Sci Eng, 1996, A 217: 401 - 406.

[9] Tsai A A, Kamiyama K, Kawamura Y, et al. Formation and precipitation mechanism of nanoscale Al particles in Al-Ni based amorphous alloy[J]. Acta Mater, 1997, 45 (4): 1477 - 1487.

[10] Kim Y H, Inoue A, Masumoto T. Increase in mechanical strength of Al-Y-Ni amorphous alloy by dispersion of nanoscale fcc-Al particle[J]. Mater Trans JIM, 1991, 32(4): 381 - 338.

[11] Kim Y H, Inoue A, Masumoto T. Ultrahigh tensile strength of $Al_{88}Y_2Ni_9M_1$(M= Mn or Fe) amorphous alloys containing finely dispersed FCC Al particles[J]. Mater Trans JIM, 1990, 31: 747 - 749.

[12] Shiflet G J, He Y, Poon S J. Mechanical properties of a new class of metallic glasses based on aluminum[J]. J Appl Phys, 1988, 64(12): 6863 - 6865.

[13] Gich M, Gloriant T, Surinach S, et al. Glass forming ability and crystallization processes within Al-Ni-Sm system[J]. Journal of Non-Crystalline Solids, 2001, 289: 214 - 220.

[14] Greer A L. Crystallization of amorphous alloys[J]. Metall Mater Trans, 1996, 27(3): 549 - 556.

[15] Wu R I, Wilde G, Perepezko J H. Glass formation and primary nanocrystallization in Al-base metallic glasses [J]. Mater Sci Eng, 2001, A301(1): 12 - 23.

[16] Inoue A. Amorphous, nanoquasicrystalline and nanocrystalline alloys in Al-based systems[J]. Progress in Materials Science, 1998, 43: 365 - 415.

[17] Inoue A, Kimura H. Fabrications and mechanical properties of bulk amorphous, nanocrystalline, nanoquasicrystalline alloys in aluminum-based system[J]. Journal of Light Metals, 2001, 10(1): 31 - 41.

[18] Bassim N, Kiminami C S, Kaufman M J. Phases formed during crystallization of amorphous $Al_{84}Y_9Ni_5Co_2$ alloy[J]. Journal of Non-Crystalline Solids, 2000, 273: 271 - 276.

[19] Philip N, Su H N. Investigation of Several Compounds in the Al-Ni-Y System[R]. Thermal Processing Technology Center, Illinois Institute of Technology, www.iit.edu

[20] Soifer L, Korin E. Effect of heatingrate on crystallization kinetics of amorphous $Al_{91}La_5Ni_4$ by DSC[J]. J Therm Analy & Calor, 1999, 56(3): 437 - 446.

[21] ZHANG Hao-yue, Brian S M. A method for determining crystallization kinetic parameters from one non-isothermal calorimetric experiment[J]. J Mater Res, 2000, 15(4): 1000 - 1007.

[22] Nataraj D, Prabakar K, Narayandass K, et al. Determination of kinetic parameters of Bi_2Se_3 thin films by computation[J]. Cryst Res Technol, 2000, 35(9): 1087 - 1094.

[23] Kempen A T W, Sommer F, Mittemeijer E J. Determination and interpretation of isothermal and non-isothermal transformation kinetics; the effective activation energies in terms of nucleation and growth[J]. J Mater Sci, 2002, 37(5): 1321 - 1332.

[24] Gaber A F, Afify N, Gadalla A, et al. Decomposition and precipitation mechanisms in supersaturated Al-Mg alloy[J]. High Temperatures-High Pressures, 1999, 31 (3): 613 - 625.

[25] Ye E, Lu K. Crystallization kinetics of Al-La-Ni amorphous alloy[J]. Journal of Non-crystalline, 2000, 262: 228 - 235.

(Edited by LONG Huai-zhong)